

## Slag parameters and sulphur partition in blast furnace hearth: Ukrainian case and international comparison

Volodymyr Shatokha

To cite this article: Volodymyr Shatokha (2021): Slag parameters and sulphur partition in blast furnace hearth: Ukrainian case and international comparison, Ironmaking & Steelmaking, DOI: [10.1080/03019233.2021.1966265](https://doi.org/10.1080/03019233.2021.1966265)

To link to this article: <https://doi.org/10.1080/03019233.2021.1966265>



Published online: 22 Aug 2021.



Submit your article to this journal [↗](#)



View related articles [↗](#)



View Crossmark data [↗](#)

---

# Slag parameters and sulphur partition in blast furnace hearth: Ukrainian case and international comparison

Volodymyr Shatokha 

National Metallurgical Academy of Ukraine, Dnipro, Ukraine

## ABSTRACT

Blast furnace ironmaking usually requires maintaining a reasonable level of hot metal desulphurization; therefore, knowledge of the complex interplay between physical properties and desulphurization potential of slag is essential for the holistic approach to the operation. Several models for predicting sulphur partition between slag and hot metal based on sulphide capacity estimation have been studied in application to the Ukrainian blast furnace. Influence of an optical basicity, as well as of  $\text{CaO/SiO}_2$  and  $\text{MgO/Al}_2\text{O}_3$  ratios on sulphur partition between slag and hot metal, was analysed. Attainment of the equilibrium partition was estimated in connection with Si content in hot metal. International comparison of blast furnace slags was conducted involving data for 25 steelworks from 16 countries covering composition, physical properties and desulphurization potential. Approaches to optimization of slag composition are discussed, considering the tradeoff between enhancing slag's desulphurization capacity and keeping its physical properties favourable to smooth and productive operation.

## ARTICLE HISTORY

Received 31 May 2021  
Accepted 6 August 2021

## KEYWORDS

Blast furnace ironmaking; desulphurization; sulphide capacity; sulphur partition; slag; hot metal; viscosity; optimization

## Introduction

The optimization of blast furnace slag composition is essential for smooth operation and hot metal quality. The discussions about optimal slag parameters usually focus on viscosity and desulphurization potential. Stability of slag properties against unforeseen deviations in the blast furnace hearth thermal conditions or in raw materials' chemistry is another essential aspect of optimization. Noteworthy, viscosity affects diffusion at slag–metal interface, thus determining the efficiency of sulphur partition between slag and hot metal, whereas both physical properties and the rate of chemical reactions are subject to thermal conditions in the hearth. Given the complexity of slag–metal–gas interactions and the diversity of general operational conditions (including slag compositions) applied in blast furnace practice across the world, the recommendations on slag parameters offered in various studies often apply to the particular conditions related to composition and specific consumption of raw materials. Along with basicity, reflected via various indices, the effect of  $\text{Al}_2\text{O}_3$ ,  $\text{MgO}$  and their proportion on sulphur partition is often considered (other oxides' effects have also been studied but not covered in this paper).

Choice of slag parameters usually involves the following options:

- high desulphurization potential of slag coupled with its satisfactory physical properties aiming at feasibly low sulphur content in tapped hot metal (external desulphurization still can be applied – for example, to meet specific requirements);
- satisfactory desulphurization potential of slag coupled with its good physical properties usually followed by external desulphurization of hot metal.

The choice depends upon many factors (e.g. sulphur content in fuel and raw materials, availability of external desulphurization and so on) and affects productivity, energy consumption and economics of ironmaking. Therefore, knowledge of the complex interplay between slag's physical properties and desulphurization potential is essential for the holistic approach to the blast furnace operation. This paper aims to assess the aspects of sulphur partition between molten slag and hot metal in the Ukrainian blast furnace and to analyse how local slag parameters differ from those encountered in other regions.

## Specific aspects of blast furnace operation in Ukraine

Major iron ore source in Ukraine is the Kryvyi Rih deposit. Specific features of this deposit are discussed elsewhere [1]. Iron ores and concentrates of Kryvyi Rih contain large amounts of silica, resulting in a relatively low content of iron and high content of silica in agglomerated products: 48.6–54.2% Fe and 8.0–9.6%  $\text{SiO}_2$  in fluxed sinter (with  $\text{CaO/SiO}_2$  ratio around 1.3), 62.1–64.6% Fe and 4.7–8.5%  $\text{SiO}_2$  in fluxed pellets ( $\text{CaO/SiO}_2$  around 0.5) [2]. Local coking grade coals are highly sulphurous, though the average share of imported coals in the coking mix recently reached 70–75% [3], thus reducing sulphur content in coke at some enterprises to around 0.9% [4]. Operation with high desulphurization potential of slag is usually applied to meet the requirements to hot metal (HM) quality. To manage unstable composition of the supplied raw materials and keep slag composition within desirable range, raw limestone is often used with consumption in the range of 20–80 kg/t-HM). Mentioned above factors result in high slag yield – usually around 450 kg/t-HM. The presence of high amounts of slag in bosh and

hearth reduces gas permeability and requires more frequent tapping followed by insufficient utilization of slag's desulphurization potential.

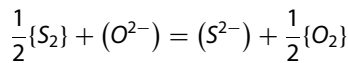
## Methodology

### Slag sulphide capacity and sulphur partition coefficient

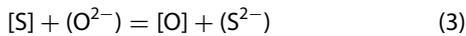
In the molten blast furnace slag, sulphur occurs as sulphide ion ( $S^{2-}$ ) [5]. Sulphur partition between slag and metal depends upon the slag to metal ratio and the sulphide capacity of the slag. Richardson and Fincham [6] defined slag sulphide capacity based on the equilibrium at slag–gas interface as follows:

$$C_S = (S) \cdot \left( \frac{P_{O_2}}{P_{S_2}} \right)^{1/2} = K \left( \frac{a_{O^{2-}}}{f_{S^{2-}}} \right), \quad (1)$$

where:  $(S)$  is sulphur content in slag (%);  $P_{O_2}$ ,  $P_{S_2}$  are partial pressures of respected gases;  $a_{O^{2-}}$  is oxygen activity in slag;  $f_{S^{2-}}$  is sulphur activity coefficient in slag;  $K$  is the equilibrium constant of the reaction ( $\{..$  and  $\{..$ ) denote substances in gas and slag, respectively)



Turkdogan and Fruehan [5] estimated sulphide capacity based on the equilibrium at slag–metal interface ( $\{..$  denotes substances in metal):



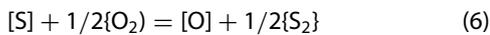
$$C'_S = (S) \frac{[a_O]}{[a_S]}, \quad (4)$$

where  $[a_O]$  and  $[a_S]$  are activities of respected elements in metal.

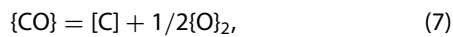
The relationship between the two estimations is described by the equation

$$C_S = \frac{C'_S}{K_{OS}} \quad (5)$$

where  $K_{OS}$  is the equilibrium constant of the reaction.



Kulikov [7], considering a reaction



elaborated the following equation for activity of carbon in liquid iron  $[a_C] = 1$

$$\lg C_S = \lg L_S^0 \frac{P_{CO}}{f_{[S]}} + \frac{780}{T} - 5.6, \quad (8)$$

where:  $L_S^0 = (S)/[S]$  is an equilibrium sulphur partition coefficient calculated as a ratio of sulphur mass concentrations in slag  $(S)$  and metal  $[S]$ ;  $f_{[S]}$  is the activity coefficient of sulphur in liquid iron.

For  $T = 1723K$  (1450°C) Equation (8) can be simplified as follows:

$$L_S^0 = 1.4 \cdot 10^5 \frac{f_{[S]}}{P_{CO}} \cdot C_S, \quad (9)$$

Based on the experimental data on equilibrium in the system 'iron – slag – graphite – CO gas' Kulikov [7] obtained

the following empirical equation:

$$\lg \frac{L_S^0}{f_{[S]}} = 2.55B' - 2.07 \quad (10)$$

where  $B'$  is basicity coefficient estimated as:

$$B' = \frac{\text{CaO} + \text{MgO}}{\text{SiO}_2 + 0.6\text{Al}_2\text{O}_3 - ((\text{CaO} + \text{MgO}/\text{SiO}_2) - 1.19)} \quad (11)$$

Combination of thermodynamic data (9) and empiric model (10) results in

$$\lg C_S = 2.55 \times B' - 7.23 \quad (12)$$

Values delivered by Equation (9) far exceed the industrial data; therefore, the following, rather arbitrarily obtained, equation was proposed [7] for approximate estimation of the sulphur partition coefficient in blast furnace hearth

$$L_S \approx 5 \cdot 10^4 \frac{f_{[S]}}{P_{CO}} \cdot C_S \quad (13)$$

Like other similar equations available in literature, Equation (12) in combination with Equation (13) enables estimation of sulphur partition for a certain slag composition expressed by the basicity index. Although basicity is extremely widely used, absence of consensus in a definition of its quantitative expression was pointed out by many researchers. Sommerville and Yang [8] argue that ratios devised for basicity estimation, compiled by Mills [9], have limited scope of application, whereas an optical basicity (a concept elaborated by Ingram and Duffy [10]) can be trusted as a more comprehensive measure of basicity.

In numerous works (e.g. [11–13]) the applicability of optical basicity as the comprehensive characteristic of slag composition was convincingly proven for various conditions of operation. Critical opinions are also noted (e.g. [14,15]), in particular, pointing out that opacity of transition metals' oxides such as FeO и MnO in ultraviolet spectral region disables experimental determination of their optical basicity. To overcome this, Sosinsky and Sommerville [11] proposed indirect estimation of optical basicity based on experimental data on the sulphide capacity of slags containing such oxides. Duffy [16] developed a method applying data on refractivity and density of transition metals' silicates and aluminates. However, the estimated optical basicity for MnO and FeO varies in a wide range. In this study, the values recommended by Sommerville and Yang [8] summarized in Table 1 are used.

Optical basicity of multi-component oxide system is estimated as

$$\Lambda = \sum_{i=1}^n X_i \cdot \Lambda_i, \quad (14)$$

where  $n$  is the total number of oxides and  $X_i$  is equivalent cationic value of oxide  $i$  determined from the equation

$$X_i = \frac{O_i \cdot N_i}{\sum_{i=1}^n O_i \cdot N_i}, \quad (15)$$

**Table 1.** Optical basicity ( $\Lambda$ ) of the oxides typical for blast furnace slags (Ref. [8]).

Oxide	CaO	MgO	Al <sub>2</sub> O <sub>3</sub>	SiO <sub>2</sub>	MnO	FeO
$\Lambda$	1.00	0.85	0.65	0.48	0.95	0.93

where  $O_i$  is a number of oxygen atoms in the molecule of oxide  $i$  and  $N_i$  is the mole share of the same oxide.

Sosinsky and Sommerville [11] obtained the following empirical equation, suitable for estimating slag's sulphide capacity from its optical basicity in the temperature range of 1400–1700°C:

$$\lg C_S = (22690 - 54640 \times \Lambda) \times T + 43.6 \times \Lambda - 25.2. \quad (16)$$

Young et al. [13] show that the relationship between  $\lg C_S$  and  $\Lambda$  is not linear; hence Equation (16) undervalues  $C_S$  of high basicity slags. Two empiric equations have been proposed for different basicity ranges. For the range of  $\Lambda < 0.8$ , relevant to blast furnace slags, the following was adopted:

$$\begin{aligned} \lg C_S = & -13.913 + 42.84 \times \Lambda - 23.82 \times \Lambda^2 \\ & - (11710/T) - 0.02223 \times (\text{SiO}_2) - 0.02275 \\ & \times (\text{Al}_2\text{O}_3), \end{aligned} \quad (17)$$

where  $(\text{Al}_2\text{O}_3)$ ,  $(\text{SiO}_2)$  are concentrations of oxides in slag in mass %.

Over the years, many researchers have developed several other sulphide capacity models. These developments are summarized, in particular, by Ma et al. [17], hence this paper does not attempt a more comprehensive review.

For practical industrial purposes, it is reasonable to not only estimate sulphide capacity but also predict sulphur partition coefficient. From the equation for the equilibrium constant of the reaction (6)

$$\lg K_{OS} = -\frac{935}{T} + 1.375 \quad (18)$$

and using Equations (4) and (5), Young et al. [13] elaborated the following equation:

$$\lg \frac{(S)}{[a_S]} = -\frac{935}{T} + 1.375 + \lg C_S - \lg [a_O]. \quad (19)$$

Sulphur activity in liquid iron can be calculated from:

$$[a_S] = [S] \times f_{[S]}. \quad (20)$$

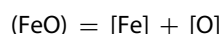
From the above, sulphur partition coefficient can be expressed as:

$$L_S = \frac{(S)}{[S]} = f_{[S]} \cdot 10^{-\frac{935}{T} + 1.375 + \lg C_S - \lg [a_O]} \quad (21)$$

Sulphur activity coefficient in low manganese liquid iron can be calculated using the following equation [7]

$$\lg f_{[S]} = -\frac{1300}{T} - 1.473 + 0.047 \cdot [Si] + 0.0024 \cdot [Si]^2 \quad (22)$$

Venkatadri et al. [18] estimated oxygen activity in liquid iron from the reaction



$$\lg K = \lg \frac{[a_O]}{a_{\text{FeO}}} = -\frac{6320}{T} + 2.734 \quad (23)$$

considering that in blast furnace slags  $a_{\text{FeO}} = N_{\text{FeO}}$  [19].

However, estimation of oxygen activity in liquid metal from the equilibrium of the Reaction (23) using the industrial slag's data has a drawback: inefficient separation of iron beads from the slag causes errors in estimation of FeO content. Application of the above equations to the models by Sosinsky and Sommerville [11] and Young et al. [13]

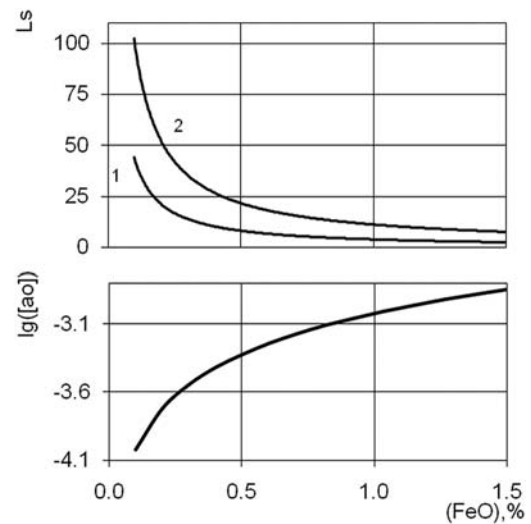


**Figure 1.** Effect of FeO content in slag on oxygen activity in liquid iron and sulphur partition coefficient estimated using the models by Sosinsky and Sommerville – 1 [11] and Young et al. – 2 [13].

demonstrates (Figure 1) that even slight deviation of FeO content in slag, especially in the most relevant to blast furnace slags range from 0.2% to 0.6%, drastically affects partition coefficient (slag composition typical for Ukraine was taken with 1.2 CaO/SiO<sub>2</sub>, 6% MgO, 8% Al<sub>2</sub>O<sub>3</sub>;  $T = 1723\text{K}$ ). Therefore, considering possible errors in FeO estimation, application of Equation (23) for estimating oxygen activity in liquid metal may cause substantial inaccuracy.

In contrast to FeO, the accuracy of MnO content in slag for low manganese hot metal production shall not be essentially affected by the presence of iron beads in slag. Young and Cripps Clark [20] proposed the following reaction as an indicator for oxygen activity estimation



defining MnO activity in liquid slag from the equation

$$a_{\text{MnO}} = 10^{-3}(\text{MnO}) \cdot \left( 1.6 + 5.9 \frac{(\text{CaO}) + 1.4(\text{MgO})}{(\text{SiO}_2)} \right). \quad (25)$$

The value of Mn activity coefficient can be defined from Wagner's equation [21] using the first order interaction parameters ( $e_{\text{Mn}}^{\text{C}} = -0.07$ ;  $e_{\text{Mn}}^{\text{Si}} = 0$ ;  $e_{\text{Mn}}^{\text{Mn}} = 0$ ;  $e_{\text{Mn}}^{\text{P}} = -0.035$ ;  $e_{\text{Mn}}^{\text{S}} = -0.043$ )

$$\lg f_{[\text{Mn}]} = e_{\text{Mn}}^{\text{C}}[\text{C}] + e_{\text{Mn}}^{\text{P}}[\text{P}] + e_{\text{Mn}}^{\text{S}}[\text{S}], \quad (26)$$

Oxygen activity can be calculated as  $[a_O] = a_{\text{MnO}}/[a_{\text{Mn}}] \cdot K_{\text{Mn}}$ , where  $[a_{\text{Mn}}] = [\text{Mn}] \cdot f_{[\text{Mn}]}$  and  $K_{\text{Mn}}$  is estimated as follows [20]

$$\lg K_{\text{Mn}} = \frac{12760}{T} - 5.5. \quad (27)$$

### Industrial data

Daily average industrial slag and metal compositions data have been collected at a single blast furnace in Ukraine with a designed capacity of 5000 t-HM per day. To address a wide range of operational conditions, data on hot metal and slag compositions have been collected for a six-month period, including episodes when the operation substantially deviated due to various reasons. Outliers have been excluded using standard statistical procedure. The ranges of the

**Table 2.** Range of hot metal and slag compositions, mass %.

Hot metal				Slag					
Si	Mn	S	P	CaO	SiO <sub>2</sub>	MgO	Al <sub>2</sub> O <sub>3</sub>	FeO	MnO
0.48–1.79	0.18–0.31	0.014–0.069	0.070–0.095	44.8–49.2	37.5–43.6	3.4–7.3	5.2–9.6	0.26–0.57	0.21–0.69

deviations in slag and hot metal compositions (after exclusion of outliers) are shown in Table 2. Hot metal carbon content and temperature have not been measured permanently and were assumed as 4.5% and 1450°C, respectively, based on the average data available from plant laboratory. Similar to other researchers (as summarized by Wang et al. [22]), considering the conditions at the interface between slag and carbon saturated iron, partial pressure  $P_{CO}$  was taken as 1 atmosphere.

## Results and discussion

### Validation of sulphide capacity models against statistic data

Figure 2 demonstrates the  $L_s$  curves calculated according to methods analysed above and plotted against the measured partition coefficient. Noteworthy, even though the equilibrium values (denoted as [7] eq) of partition coefficient estimated using Kulikov's Equation (9) far exceed plant data, their linear approximation curve is nearly parallel to an ideal plot. In contrast, curves obtained for the equations intended to estimate real partition coefficient in all three analysed methods exhibit lesser slope than needed to fit the industrial data. Hence, model by Young et al. [13] overestimates  $L_s$  in low-value range while providing relatively relevant forecast for  $L_s$  values above 60, whereas models by Kulikov [7] and Sosinsky and Sommerville [11] deliver rather underestimated values and the relevance of these models' forecast deteriorates with growth of  $L_s$ .

Statistical data in Table 3 show that optical basicity, CaO/SiO<sub>2</sub> ratio and Kulikov's basicity ratio (11) have nearly equally strong correlation with  $L_s$ , whereas other ratios have weaker correlation.

Plots of  $L_s$  values – measured and estimated using various models – versus the basicity ratio CaO/SiO<sub>2</sub> are shown in Figure 3. Only the model by Young et al. [13] fits within the scatter of industrial data (greyed area) whereas the other models suit only basicity below 1.15 CaO/SiO<sub>2</sub>. Obviously, prediction of  $L_s$  could be further enhanced – for example, by adjustment of the curve delivered by Equation (17) to the local statistical data.

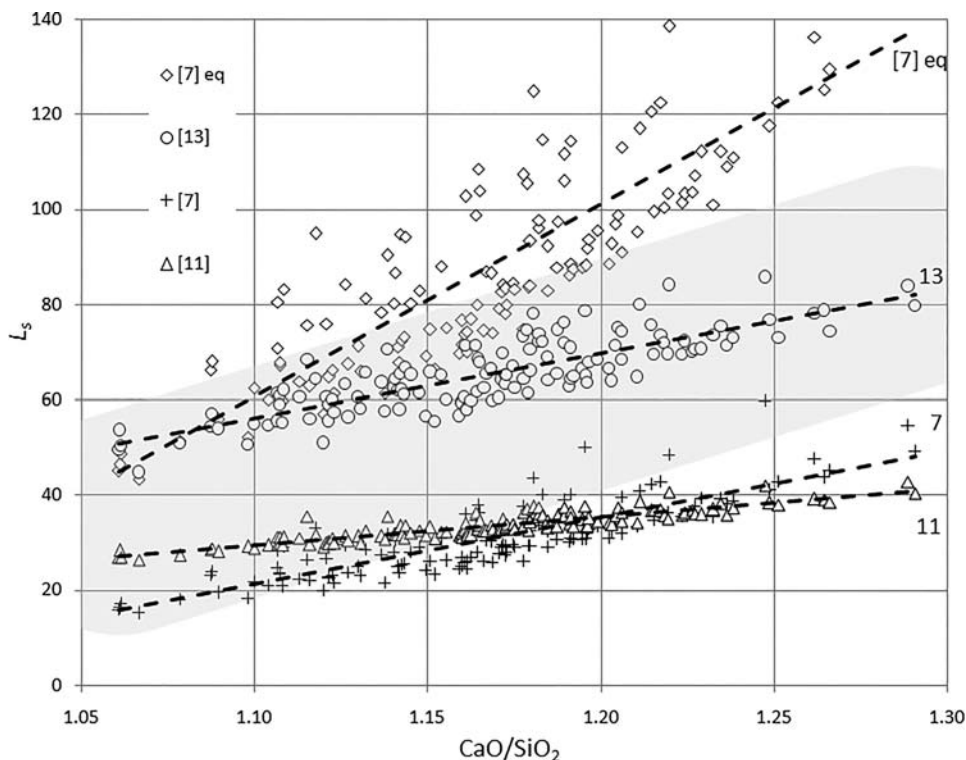
### On the deviation from equilibrium

Sulphur partition between slag and hot metal in the blast furnace depends upon the operation parameters, thermal conditions, iron and slag compositions, slag yield, etc. According to [23,24], sulphur partition is close to equilibrium, although we found no sufficient quantitative information in literature to support this opinion. To quantify the attainment of equilibrium sulphur partition in industrial conditions, following ratio was applied

$$\varepsilon = \left( \frac{L_s}{L_s^0} \right) \cdot 100\%, \quad (28)$$

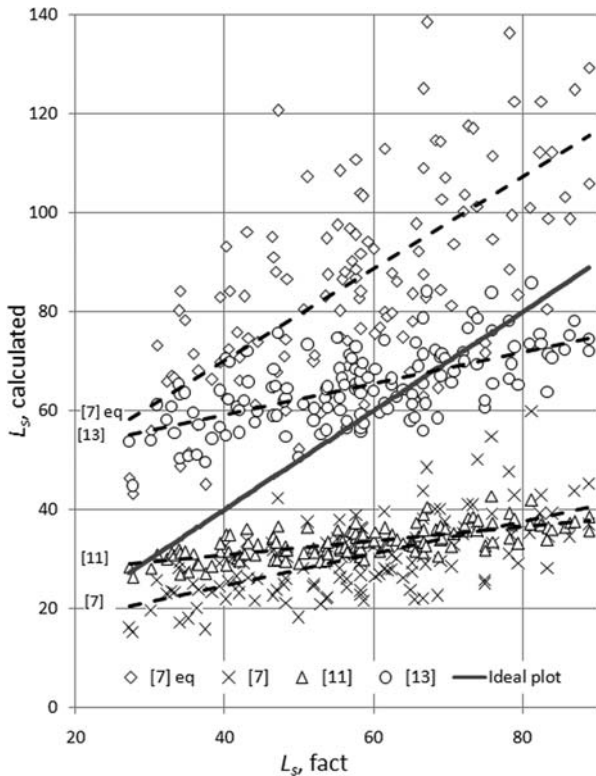
where  $L_s$  represents the plant data and  $L_s^0$  was defined using Equation (9).

The average  $\varepsilon$  value of 66% was obtained with minimum and maximum of 39% and 95%, respectively (100% means

**Figure 2.** Plot of  $L_s$  values calculated using various models versus industrial data.

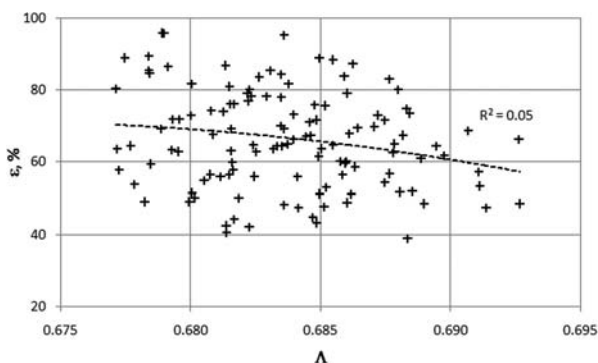
**Table 3.** Coefficients of correlation with  $L_s$ .

Indicator	CaO/SiO <sub>2</sub>	(CaO + MgO)/SiO <sub>2</sub>	(CaO + MgO)/(SiO <sub>2</sub> + Al <sub>2</sub> O <sub>3</sub> )	$\Lambda$	$B'$	[Si]
Coefficient of correlation with $L_s$	0.68	0.42	0.43	0.69	0.68	0.39

**Figure 3.** Calculated and industrial  $L_s$  values versus basicity CaO/SiO<sub>2</sub> ratio (greyed area represents the scatter of the industrial  $L_s$  values).

attainment of equilibrium). As shown in Figure 4, deviation from the equilibrium tends to grow with increased optical basicity which could mean that enhanced desulphurization potential of high basicity slag might be offset by its higher viscosity. However, as seen from the coefficient of determination, statistical significance of trend is rather poor, owing to simultaneous influence of many factors other than optical basicity. In particular, as seen from Table 2, Si content in hot metal varied significantly, indicating unstable thermal conditions.

Although the correlation between  $L_s$  and Si content in hot metal seems not very strong (Table 3); thermal conditions in the hearth (reflected in Si content) shall affect the deviation from equilibrium. To adjust industrial data to specific Si

**Figure 4.** Attainment of equilibrium sulphur partition versus slag optical basicity (industrial data,  $R^2$  – coefficient of determination).

content in hot metal, the following equation reflecting a combined effect of slag composition and Si content in hot metal (in mass %) on sulphur partition was obtained using a multiple regression analysis (multiple correlation coefficient  $R = 0.73$ )

$$L_s = -1644 + 2472 \times \Lambda + 14 \times [\text{Si}] \quad (29)$$

Effect of Si on the value of equilibrium sulphur partition coefficient ( $L_s^0$ ) is taken into account via sulphur activity coefficient in Equation (22). The results in Figure 5 show that basicity growth is followed by more substantial deviation of the sulphur partition from the equilibrium, representing a cumulative effect of simultaneous growth of  $L_s^0$  value and of slag viscosity, making attainment of equilibrium more difficult. Higher Si content in hot metal brings sulphur partition closer to equilibrium: growth of equilibrium value thanks to higher sulphur activity coefficient in hot metal (22) appears less significant than effect of elevated thermal conditions in the hearth, to which higher Si content in hot metal is usually attributed (although precise judgment would require knowledge of the hot metal temperature).

### On the optimal slag composition

Figure 6 represents the industrial  $L_s$  values in coordinates CaO/SiO<sub>2</sub> versus MgO/Al<sub>2</sub>O<sub>3</sub>. Such a presentation has two advantages over other formats required to depict a quaternary system:

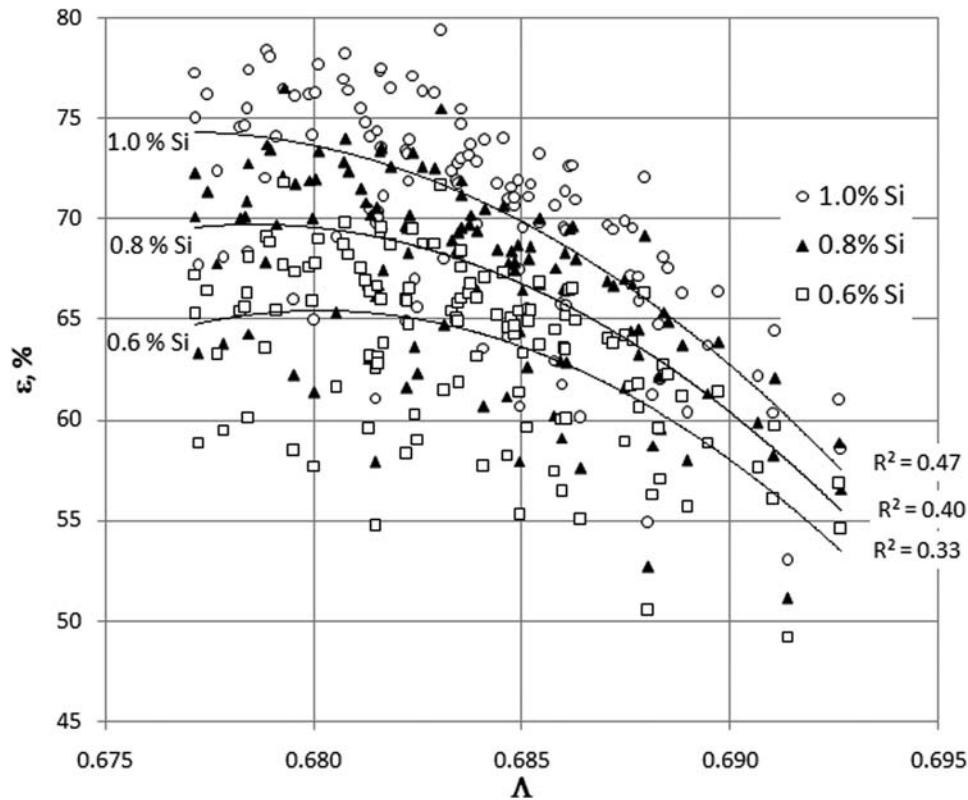
- most exact demonstration of the observed data – after adjustment into four-component system, no recalculation to fixed content of one component needed (as it shall be done in case of more usual triangular cross-section layout);
- easier setup and more straightforward reading compared with 3D format.

Figure 6 also depicts intersections of liquidus surfaces, crystallization phase fields, liquidus surface isotherms (by Ref. [25]), iso-viscosity (by Ref. [26]) and iso- $L_s$  curves for the CaO-SiO<sub>2</sub>-MgO-10% Al<sub>2</sub>O<sub>3</sub> slags. Iso- $L_s$  curves were built using the following equation derived from multiple regression analysis (multiple correlation coefficient  $R = 0.84$ )

$$L_s = -540.8 + 509.4 \times \text{CaO/SiO}_2 + 57.7 \times \text{MgO/Al}_2\text{O}_3 \quad (30)$$

Most slag compositions correspond to the Melilite and the Merwinite phase fields. These fields were defined by Osborne et al. [25] as an optimum where slag is entirely liquid and high desulphurization potential is combined with low viscosity (viscosity values below 0.5 Pa·s are considered as suitable for blast furnace operation [27,28]). Plateau-like liquidus surface in the Merwinite phase field is situated at a temperature around 1500°C, whereas liquidus surface in the Melilite phase field is slightly inclined between 1350°C and 1500°C isotherms.

Fewer slag compositions fall into dicalcium silicate phase field where the basicity growth is followed by the steep



**Figure 5.** Effect of optical basicity on the attainment of equilibrium sulphur partition for various Si content in hot metal. Industrial Ls values are adjusted to equal Si content in hot metal using equation (29);  $R^2$  – coefficient of determination.

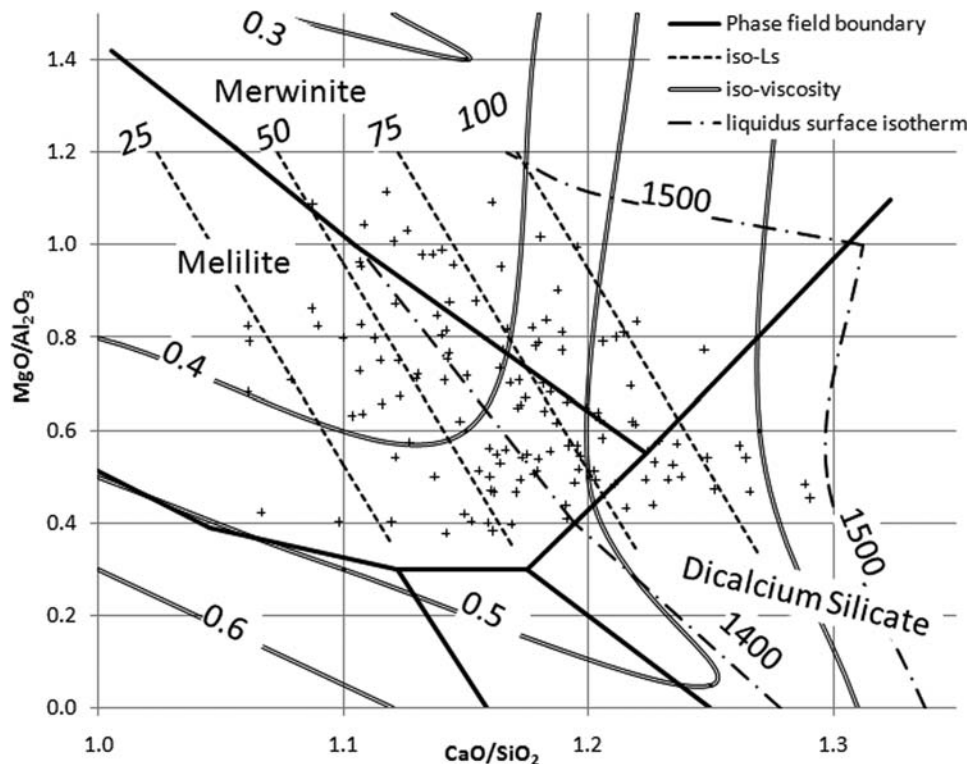


**Figure 6.** Compositions of industrial slags in  $\text{CaO-SiO}_2\text{-MgO-10\%Al}_2\text{O}_3$  diagram (viscosity in Pa s for  $1450^\circ\text{C}$ , temperature in  $^\circ\text{C}$ ).

ascent of liquidus surface towards very high temperatures. The latter field is unsuitable for stable blast furnace operation and falling of some slag compositions into this field is explained by the fact that the phase fields' boundaries and viscosities in Figure 6 correspond to  $\text{CaO-SiO}_2\text{-MgO-10\%Al}_2\text{O}_3$  system, whereas real  $\text{Al}_2\text{O}_3$  content deviated from 5.2% to 9.6%; moreover, properties of real slag are also

greatly affected by presence of sulphur, FeO and MnO in slag (so, viscosity of industrial slag shall be lower).

The positive effect of MgO on slag properties has been repeatedly confirmed for the Ukrainian conditions but, owing to the deficit of local dolomite resources, MgO content in slag is usually lesser than recommended [29,30]. In Figure 6, higher  $\text{MgO/Al}_2\text{O}_3$  ratio at constant  $\text{CaO/SiO}_2$

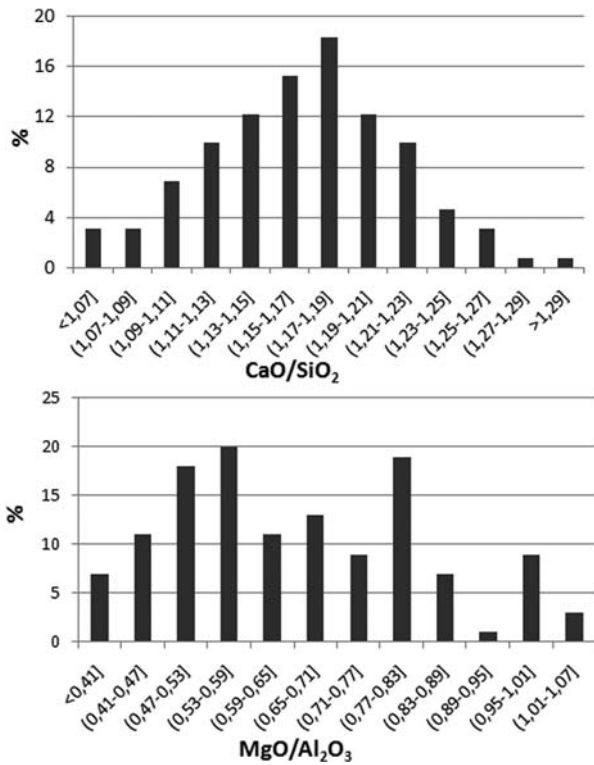


**Figure 7.** Distribution of  $\text{CaO}/\text{SiO}_2$  and  $\text{MgO}/\text{Al}_2\text{O}_3$  ratios of the industrial slags.

correspond to higher desulphurization potential and lower viscosity of slag; however, the Melilite phase field where slag has lower liquidus temperature is more favourable for ensuring sustainability of slag properties against deviations of thermal conditions in the hearth.

In contrast to basicity, which being one of the most important operational parameters closely follows normal distribution with 85% of compositions within the range from 1.09 to 1.23  $\text{CaO}/\text{SiO}_2$ , distribution of  $\text{MgO}/\text{Al}_2\text{O}_3$  demonstrates no distinct pattern thus indicating that MgO content in slag was not in managed (Figure 7).

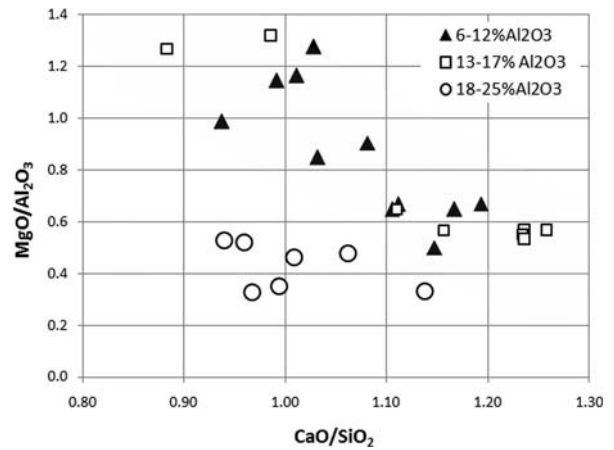


**Figure 8.** Compositions industrial slags from various regions of the world grouped by  $\text{Al}_2\text{O}_3$  content.

Discussed above allows considering slag compositions adjacent to the intersection of Melilite and Merwinite phase fields (preferably within the Melilite field) as optimal, if high desulphurization potential of slag is a target. For the dominant basicity range of 1.15–1.19  $\text{CaO}/\text{SiO}_2$  it corresponds to 0.84–0.68  $\text{MgO}/\text{Al}_2\text{O}_3$ ; however, as seen from Figure 7, large part of slag compositions are observed in much lower  $\text{MgO}/\text{Al}_2\text{O}_3$  range.

For international comparison, the data on the slag compositions for 25 steelworks representing 16 countries have been collected in literature [31–46] and shown in Figure 8. All compositions have been adjusted to equal content of MnO (0.3%) and FeO (0.4%) and recalculated to 100% of  $\text{CaO} + \text{SiO}_2 + \text{MgO} + \text{Al}_2\text{O}_3 + \text{FeO} + \text{MnO}$ . By  $\text{Al}_2\text{O}_3$  content, all slags were classified into three groups – 6–12%, 13–17% and 18–25%. By the combination of  $\text{CaO}/\text{SiO}_2$  and  $\text{MgO}/\text{Al}_2\text{O}_3$  ratios, slags with 6–17%  $\text{Al}_2\text{O}_3$  (including Ukrainian) fit into a common pattern represented with greyed area, whereas slags with 18–25%  $\text{Al}_2\text{O}_3$  (all belong to India) distinctly represent a separate group. In some countries, slag compositions

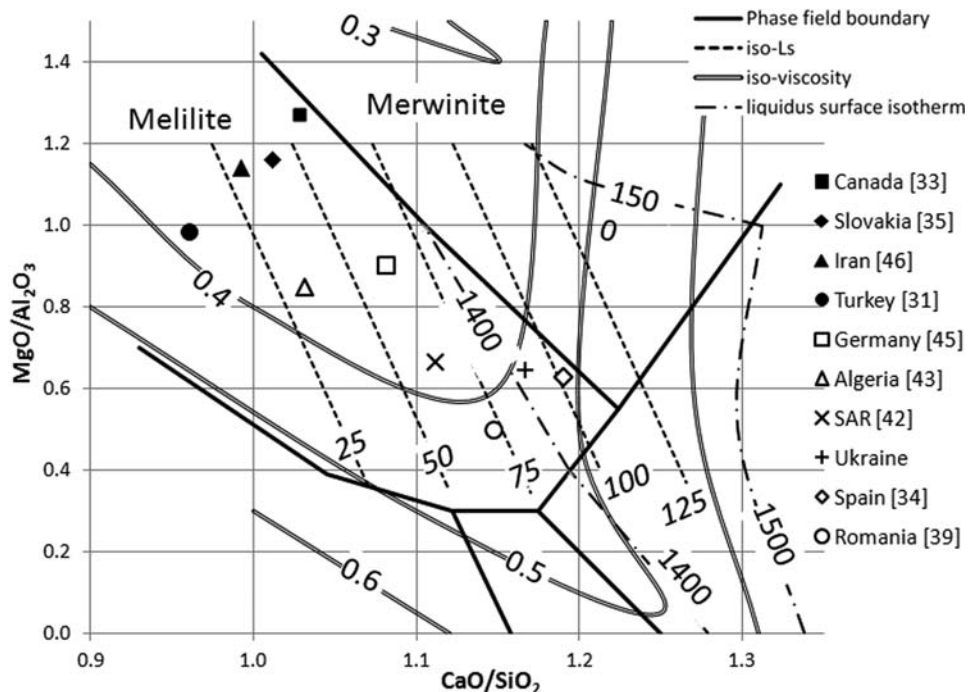


**Figure 9.** Compositions of industrial slags from various countries in  $\text{CaO}\text{-SiO}_2\text{-MgO}\text{-}10\%\text{Al}_2\text{O}_3$  diagram.

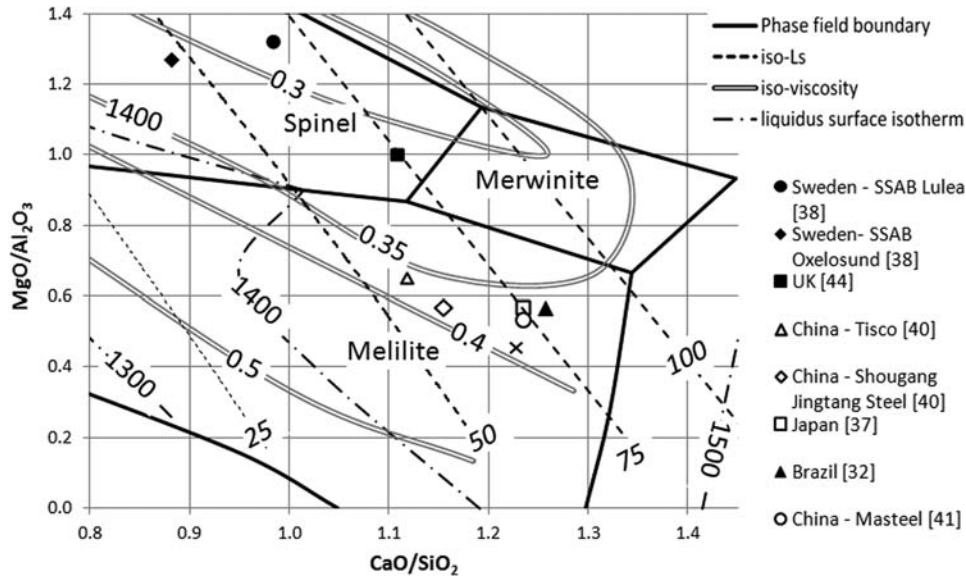


**Figure 10.** Compositions of industrial slags from various countries in  $\text{CaO}\text{-SiO}_2\text{-MgO}\text{-15\%Al}_2\text{O}_3$  diagram.

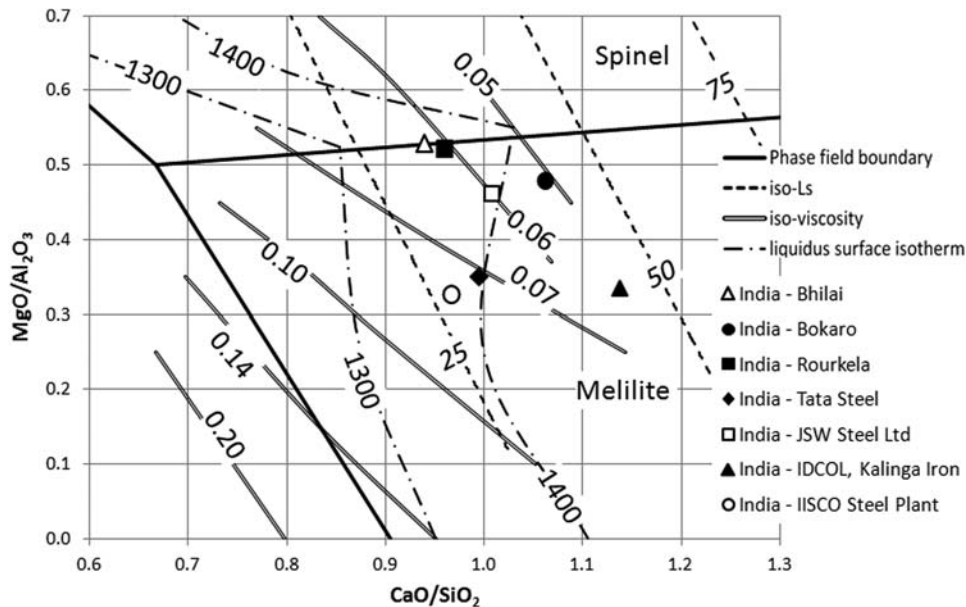


**Figure 11.** Compositions of Indian industrial slags [36] in  $\text{CaO}\text{-SiO}_2\text{-MgO}\text{-20\%Al}_2\text{O}_3$  diagram.

of different enterprises are very close; in such cases, the average values are used and further, in Figures 9–11, the names of the enterprises are denoted only when slag compositions from a single country are essentially different.

Closer look at the defined subgroups reveals the following aspects.

(1) Slags with 6–12%  $\text{Al}_2\text{O}_3$  content, including the studied Ukrainian case, fit into the Melilite phase field of the  $\text{CaO}\text{-SiO}_2\text{-MgO}\text{-10\%Al}_2\text{O}_3$  system, as shown in Figure 9. With few exceptions, slags tend to locate along the Melilite/Merwinite boundary reflecting the mentioned above tradeoff between better desulphurization and lower slag liquidus temperature. All slags are located in the area where slag has viscosity below 0.5 Pa s and most of them, with exception of Romania, Spain and Ukraine, below 0.4 Pa s. The latter three cases also correspond to slags with the highest  $L_s$  values. Noteworthy, this analysis compares slag compositions only and doesn't include

any data on sulphur partition in the referred cases, hence iso- $L_s$  values only indicatively denote desulphurization potential (e.g. sulphur input might be minor and not require high basicity slag operation or plant may operate with external desulphurization and minimization of sulphur content in tapped metal is not prioritized).

- (2) Slags with 13–17%  $\text{Al}_2\text{O}_3$  content are located in two different phase fields of  $\text{CaO}\text{-SiO}_2\text{-MgO}\text{-15\%Al}_2\text{O}_3$  system – Brazil, China and Japan in the Melilite, while Sweden and UK in the Spinel (Figure 10). All slags are very close in liquidus temperature and desulphurization potential. Slags in the Spinel field have lower viscosity – around 0.30 Pa s versus 0.35–0.40 Pa s in the Melilite field. This and next group of slags are very different by composition from the Ukrainian ones; therefore, in these two cases, iso- $L_s$  curves are determined using Equation (21) with  $C_s$  values calculated using Equation (17).
- (3) Slags with 18–25%  $\text{Al}_2\text{O}_3$  content are located in the Melilite phase field very close to an intersection with the Spinel

phase field of CaO-SiO<sub>2</sub>-MgO-20%Al<sub>2</sub>O<sub>3</sub> system – an area with low liquidus temperature and low viscosity, although desulphurization potential of slag is moderate (Figure 11).

Obviously, the choice of slag composition in each case depends upon local conditions including sulphur input with charge materials as well as availability and feasibility of external desulphurization; however, analysis of such factors exceeds the scope of current study.

## Conclusions

Sulphur partition between molten slag and hot metal in the Ukrainian blast furnace was assessed. Several sulphide capacity models have been reviewed for predicting sulphur partition between slag and hot metal in the Ukrainian industrial blast furnace. Sulphide capacity models provide generally adequate prediction. Best applicability of the model by Young et al. [13] was revealed; however, further enhancement of prediction would require tuning of the Equation (17) to local empirical data. Attainment of equilibrium in sulphur partition under the studied conditions reaches in average 66% and is favoured by lower basicity and higher content of Si in hot metal.

Reflecting the peculiarities of raw materials' quality, the blast furnaces in Ukraine operate with elevated slag yield (usually around 450 kg/t-HM) followed by more frequent tapping and insufficient utilization of the desulphurization potential of the high basicity slag. International comparison suggests that, generally, Ukrainian blast furnace slag compositions fit the optimization pattern observed in other countries where Al<sub>2</sub>O<sub>3</sub> content in slag does not exceed 12% (other countries form two distinct groups with 13–17% and 18–25% Al<sub>2</sub>O<sub>3</sub> content). Although local slag has relatively high desulphurization potential, its viscosity is substantially higher than in the majority of countries and sustainability of slag properties is vulnerable to the deviations of thermal conditions in the hearth.

## Disclosure statement

No potential conflict of interest was reported by the author(s).

## ORCID

Volodymyr Shatokha  <http://orcid.org/0000-0001-6024-0557>

## References

- [1] Stupnik M, Shatokha V. History and current state of mining in the Kryvyi Rih iron ore deposit. In: V Shatokha, editor. Iron ores. London: IntechOpen; 2021. p. 17–30.
- [2] Nesterov OS, Khamkhotko AF, Bielkova AI, et al. Updating of database and models to predict the iron ore materials properties. *Fundam Appl Prob Ferrous Metall: Collect Res. Dnipropetrovsk.* 2012;26:120–129. (in Russian). <http://dspace.nbuu.gov.ua/bitstream/handle/123456789/136319/11-Nesterov.pdf?sequence=1>.
- [3] Ukrmetprom. The results of the mining & metallurgical complex of ukraine activity in 2020. Available from: <https://www.ukrmetprom.org/the-results-of-the-mining-metallurgical-complex-of-ukraine-activity-in-2020/>.
- [4] Podkorytov AL, Kuznetsov AM, Zubenko AV, et al. Introduction of pulverized-coal injection at yenaikieiev iron and Steel works. *Steel Transl.* 2017;47(5):313–319.
- [5] Turkdogan ET, Fruehan RJ. Fundamentals of iron and steelmaking. In: RJ Fruehan, editor. The making, shaping and treating of steel. Pittsburgh: AISE Steel Foundation; 1998. p. 13–157.
- [6] Richardson FD, Fincham CJB. Sulfur in silicate and aluminate slags. *J Iron Steel Inst.* 1954;178:4–15.
- [7] Kulikov IS. Desulfurization of pig iron. Moscow: Gostechizdat; 1962; (in Russian).
- [8] Sommerville ID, Yang Y. Basicity of metallurgical slags. International congress on mineral processing and extractive metallurgy, "Minprex 2000". Melbourne: AusIMM; 2000. p. 25–32.
- [9] Mills KC. Basicity and optical basicities of slags. In: Verein Deutscher Eisenhüttenleute (VDEh), editor. Slag atlas. 2nd edition. Düsseldorf: Verlag Stahleisen GmbH; 1995. p. 9–19.
- [10] Ingram MD, Duffy JA. Transition metal ions as spectroscopic probes for detection of network structure in novel inorganic glasses. *J Am Ceram Soc.* 1970;53(6):317–328.
- [11] Sosinsky DJ, Sommerville ID. The composition and temperature dependence of the sulfide capacity of metallurgical slags. *Metall Trans.* 1986;17 B:331–336.
- [12] Sommerville ID. The measurement, prediction and use of capacities of metallurgical slags. Proc. 4th Int. Conf. on Injection metallurgy "scaninject IV," Luleå, Sweden, June 11–13, 1986, Luleå: MEFOS, 1986, 8.1–8.21.
- [13] Young RW, Duffy JA, Hasal CJ, et al. Use of optical basicity concept for determining phosphorus and sulfur slag-metal partitions. *Ironmak Steelmak.* 1992;19:201–219.
- [14] Sichen D, Nilson R, Seetharaman S. A mathematical model for estimation of sulfide capacities of multi component slags. *Steel Res.* 1995;66:458–462.
- [15] Nakamura T, Yokohama T, Toguri JM. Limitations in the metallurgical application of optical basicity. *ISIJ Int.* 1993;33:201–209.
- [16] Duffy JA. Use of refractivity data for obtaining optical basicities of transition metal oxides. *Ironmak Steelmak.* 1989;16:426–428.
- [17] Ma X, Chen M, Xu H, et al. Sulphide capacity of CaO-SiO<sub>2</sub>-Al<sub>2</sub>O<sub>3</sub>-MgO system relevant to low MgO blast furnace slags. *ISIJ Int.* 2016;56:2126–2131.
- [18] Venkatadri AS, Srinivasan CR, Gupta SK. Prediction of sulfide capacity of blast furnace slags. *Scand J Metall.* 1989;18:89–94.
- [19] Tsuchiya N, Tokuda M, Ohtani M. The transfer of silicon from the gas phase to molten iron in the blast furnace. *Metall Trans.* 1976;7B:315–320.
- [20] Young DJ, Cripps Clark CJ. Sulphur partition in blast furnace hearth. *Ironmak Steelmak.* 1980;7:209–214.
- [21] Wagner C. Thermodynamics of alloys. Mass: Addison-Wesley; 1952.
- [22] Zhenyang W, Jianliang Z, Gang A, et al. Analysis on the oversize blast furnace desulfurization and a sulfide capacity prediction model based on congregated electron phase. *Metall Mater Trans B.* 2016;47:127–134.
- [23] Okhotskiy VB. On the equilibrium in the metal-slag system for the blast furnace process. *Metallurgicheskaya i Gornorudnaya Promyshlennost.* 1994;4:1–3. (in Russian).
- [24] Venkatradi AS, Bell HB. Sulphur partition between slag and metal in the Iron Blast furnace. *J Iron Steel Inst.* 1969;207:1110–1114.
- [25] Osborn EF, DeVries RC, Gee KH, et al. Optimum composition of blast furnace slag as deduced from liquidus data for the quaternary system CaO-MgO-Al<sub>2</sub>O<sub>3</sub>-SiO<sub>2</sub>. *Trans AIME J Met.* 1954;200:33–45.
- [26] Gultiyar II. Effect of alumina on the viscosity of slag system calcium oxide – magnesium oxide – silica. *Izvestiya AN SSSR. Metallurgiya i Toplivo.* 1962;5:52–65. (in Russian).
- [27] Voskoboinikov VG, Dunayev NE, Mikhalevich A.G. properties of molten blast furnace slags. Moscow: Metallurgiya; 1975; (in Russian).
- [28] Chen M, Zhang D, Kou M, et al. Viscosities of iron blast furnace slags. *ISIJ Int.* 2014;54:2025–2030.
- [29] Shatokha VI. Selection of rational composition of blast furnace slag. *Metallurgicheskaya i Gornorudnaya Promyshlennost.* 2000;1–2:33–34. (in Russian).
- [30] Togobitskaya DN, Khamkhotko AF, Stepanenko DA. Relation of viscosity and crystallization temperature of blast furnace slags with their mineralogical composition. *Fundam Appl Prob Ferrous Metall: Collect Res Works.* Dnipropetrovsk. 2010;21:108–116. (in Russian).
- [31] Gesoglu M, Guneyisi E, Oz H. Properties of lightweight aggregates produced with cold-bonding pelletization of fly ash and ground granulated blast furnace slag. *Mater Struct.* 2012;45:1535–1546.

- [32] Melo Neto AA, Cincotto MA, Repette W. Drying and autogenous shrinkage of pastes and mortars with activated slag cement. *Cem Concr Res.* 2008;38:565–574. doi:10.1016/j.cemconres.2007.11.002.
- [33] Kermani M, Hassani FP, Aflaki E, et al. Evaluation of the effect of sodium silicate addition to mine backfill, Gelfill – part 1. *J Rock Mech Geotech Eng.* 2015;7:266–272.
- [34] Rivera RA, Sanjuán MA, Martín DA. Granulated blast-furnace slag and coal fly ash ternary portland cements optimization. *Sustainability.* 2020;12:5783.
- [35] Baricová D, Pribulová A, Demeter P, et al. Utilizing of the metallurgical slag for production of cementless concrete mixtures. *Metalurgija.* 2012;51:465–468.
- [36] SLAG – IRON AND STEEL Indian Minerals Yearbook 2018 (Part-II: Metals and Alloys) 57th Edition. GOVERNMENT OF INDIA. MINISTRY OF MINES.
- [37] Isawa T. Update of iron and steel slag in Japan and current developments for valorization. In: 3rd International Slag Valorisation Symposium; Leuven, 2013 19–20 March, pp. 87–98. Available from: [https://www.slag-valorisation-symposium.eu/2013/images/papers/s1\\_4\\_Isawa.pdf](https://www.slag-valorisation-symposium.eu/2013/images/papers/s1_4_Isawa.pdf)
- [38] Westholm LJ. The use of blast furnace slag for removal of phosphorus from wastewater in Sweden – a review. *Water (Basel).* 2010;2:826–837.
- [39] Nicula LM, Corbu O, Iliescu M. Using the blast furnace slag as alternative source in mixtures for the road concrete for a more sustainable and cleaner environment. *Rev Română de Materiale/Romanian J Mater.* 2020;50:545–555.
- [40] Kexin J, Jianliang Z, Chunlin C, et al. Operation characteristic of super-large blast furnace slag in China. *ISIJ Int.* 2017;57:983–988.
- [41] Wu X, Wang H, Li L, et al. Synthesis of cordierite powder from blast furnace slag trans. *Ind Ceram. Soc.* 2013;72:197–200.
- [42] Muller J, Erwee M. Blast furnace control using slag viscosities and liquidus temperatures with phase equilibria calculations. In: RT Jones, P den Hoed, editor. *Southern african pyrometallurgy, Johannesburg.* 2011. p. 309–326. <https://www.saimm.co.za/Conferences/Pyro2011/309-Muller.pdf>.
- [43] Rouabah K, Zergua A, Beroual A, et al. Recovery and use of blast furnace slag in the field of road construction in Algeria. *Open J Civ Eng.* 2013;3:113–118.
- [44] Bougara A, Lynsdale C, Milestone NB. Reactivity and performance of blast furnace slags of differing origin. *Cem Concr Compos.* 2010;32:319–324.
- [45] Senk D, Firsbach F. Quality and use of blast furnace slags. In: 3rd International VDEh-Seminar: Iron Making; Cologne, Germany, March 2015, [https://www.researchgate.net/publication/289525879\\_Quality\\_and\\_Use\\_of\\_Blast\\_Furnace\\_Slags](https://www.researchgate.net/publication/289525879_Quality_and_Use_of_Blast_Furnace_Slags)
- [46] Nilforoushan MR, Otraj S. The study of Ion adsorption by amorphous blast furnace slag. *Iran J Chem Chem Eng.* 2015;34:57–64.

## Appendix

### Notations

### Symbols

$C_s$	– sulphide capacity;
$P_i$	– partial pressures of gas $i$ ;
$a_i$	– activity of specie $i$ ;
$f_i$	– activity coefficient of specie $i$ ;
$X_i$	– equivalent cationic value of oxide $i$ ;
$O_i$	– number of oxygen atoms in the molecule of oxide $i$ ;
$N_i$	– mole share of oxide $i$ in slag;
$L_s^e$ and $L_s$	– equilibrium and observed sulphur partition coefficient, respectively;
$e_{Mn}^i$	– first order interaction parameter of element $i$ and manganese in molten iron;
$\varepsilon$	– degree of attainment of equilibrium sulphur partition;
$\Lambda$	– optical basicity;
$K$	– chemical equilibrium constant;
$T$	– temperature in K.

### Parentheses

{..}, (..) and [..] denote substances in gas, molten slag and molten iron, respectively.